Bioelectromagnetics 32:234–242 (2011)

Exposure Assessment in Front of a Multi-Band Base Station Antenna

Bor Kos,[1,2] Blaž Valič,[2] Tadej Kotnik,[1] and Peter Gajšek[2]*

[1]*Faculty of Electrical Engineering, University of Ljubljana, Ljubljana, Slovenia*
[2]*INIS – Institute of Non-ionizing Radiation, Ljubljana, Slovenia*

This study investigates occupational exposure to electromagnetic fields in front of a multi-band base station antenna for mobile communications at 900, 1800, and 2100 MHz. Finite-difference time-domain method was used to first validate the antenna model against measurement results published in the literature and then investigate the specific absorption rate (SAR) in two heterogeneous, anatomically correct human models (Virtual Family male and female) at distances from 10 to 1000 mm. Special attention was given to simultaneous exposure to fields of three different frequencies, their interaction and the additivity of SAR resulting from each frequency. The results show that the highest frequency—2100 MHz—results in the highest spatial-peak SAR averaged over 10 g of tissue, while the whole-body SAR is similar at all three frequencies. At distances >200 mm from the antenna, the whole-body SAR is a more limiting factor for compliance to exposure guidelines, while at shorter distances the spatial-peak SAR may be more limiting. For the evaluation of combined exposure, a simple summation of spatial-peak SAR maxima at each frequency gives a good estimation for combined exposure, which was also found to depend on the distribution of transmitting power between the different frequency bands. Bioelectromagnetics 32:234–242, 2011.

Key words: occupational RF exposure; multi-band base station; finite-difference time-domain method; whole-body SAR; spatial-peak SAR

INTRODUCTION

Maintenance workers and technicians in the mobile communications industry often have to work in the vicinity of mobile communication base station antennas and it is not always possible to turn off all transmitters at a site. Occasionally, other workers also have to perform their tasks close to base station antennas, sometimes without the knowledge of the base station operator. Because the strongest fields are found near base station antennas, an exposure assessment is needed for all those who may come close to them. With the Directive 2004/40/EC coming into effect, all employers in the European Union will be required to assess the levels of electromagnetic fields (EMF) to which their workers are exposed. Because multi-band antennas for mobile communications are ever more widespread, in this study we present a study on how electromagnetic sources of this type interact with the human body, with the focus on compliance testing with basic restrictions.

Exposure limits are defined in the International Commission on Non-Ionizing Radiation Protection (ICNIRP) Guidelines [ICNIRP, 1998] and the Institute of Electrical and Electronics Engineers (IEEE) standard C95.1 [IEEE, 2006]. In the frequency band of Global System for Mobile Communications (GSM) and Universal Mobile Telecommunications System (UMTS) mobile networks ranging from 900 to 2100 MHz, both use the specific absorption rate or SAR—the measure of absorbed power per mass of tissue—as the dosimetric quantity. Since SAR in a human body cannot be measured non-invasively, experimental assessment has to be performed on phantoms—plastic shells approximating the shape of the human body filled with conductive liquid [CENELEC, 2002]. A robotic measurement setup is usually used to scan the volume of the phantom for highest SAR values. As an alternative, numerical assessment allows investigating SAR in a more realistic, heterogeneous model of the body, with finite-difference time-domain (FDTD) method being the most commonly used [Hand, 2008]. Several 3D heterogeneous anatomical models have been constructed either from cryosection [Ackerman, 1998] or

Grant sponsor: Slovenian Research Agency (Project L7-2231).

*Correspondence to: Peter Gajšek, INIS, Pohorskega bataljona 215, SI-1000 Ljubljana, Slovenia. E-mail: peter.gajsek@inis.si

Received for review 10 February 2010; Accepted 16 November 2010

DOI 10.1002/bem.20640
Published online 22 December 2010 in Wiley Online Library (wileyonlinelibrary.com).

from images of high-resolution computed tomography or magnetic resonance imaging [Dimbylow, 1997; Christ et al., 2010].

A number of studies on near-field exposure to base station antennas have been published, ranging from measurement of fields [Cooper et al., 2002] and numerical calculation of SAR and EMF [Martinez-Burdalo et al., 2005; van Wyk et al., 2005; Lacroux et al., 2008] to estimation formulas based on antenna parameters [Faraone et al., 2000; Thors et al., 2008]. All of these studies have investigated the exposure to one frequency at a time. In realistic settings, however, there are often several transmitters at one site, operating at different frequencies simultaneously. The most interesting case is three-band antennas, which combine all the three common mobile communication frequencies (900, 1800, and 2100 MHz) in a single panel antenna and are widely used by network providers. Because the EMF of all three frequencies are radiated simultaneously in both space and time, a combined exposure evaluation gives a more complex and complete picture than if the exposure to each frequency is assessed alone.

In this study, we present a model of a commercially available three-band antenna and its interaction with different heterogeneous human models. We also assess the most important factors limiting the safety distance and compare our results with previously published data. The goals of this study were to investigate two different approaches for evaluating simultaneous exposure to multiple frequencies: to evaluate their practical usability, and to determine their influence on the final compliance regions for base station antennas.

MATERIALS AND METHODS

Numerical Computation

We used the SEMCAD X version 14 (Schmid & Partner Engineering, Zurich, Switzerland) platform for modeling and simulations. The FDTD is very suitable for evaluating human exposure to radiofrequency EMF as the computational cost rises linearly with the size of the problem. In all cases, the human body and the box phantom were discretized to a resolution of 2 mm $\times$ 2 mm $\times$ 2 mm as a suitable trade-off between accuracy and computational cost [Gosselin et al., 2009]. In FDTD simulations, the number of cells per wavelength in the medium has an effect on wave propagation speed and field attenuation. At the highest frequency used in our simulations (2100 MHz), the tissue with the smallest number of cells per wavelength is the gallbladder (8.5 cells per wavelength). However, the number of cells per wavelength in tissues closer to the surface, such as muscle, skin, fat etc., which get the bulk of EMF exposure, is higher than 9.5. Each simulation was run for 20 periods of the central frequency to ensure that the wave propagated throughout the entire computational domain as well as to allow the simulation to reach a steady state.

Antenna Model and Validation

A three-band panel base station antenna (Kathrein 742 265, Kathrein; Scala Division, Medford, OR) was evaluated. It has two sets of radiating elements, one for 900 MHz GSM with six radiating elements, and another for 3G UMTS at 2100 MHz and GSM at 1800 MHz with 11 radiating elements. All the three bands can be used simultaneously by using appropriate combiners. We modeled the geometry based on an actual antenna that has been taken out of use and dismantled; we were able to model the array and the internal structure as shown in Figure 1. The metal parts were modeled as perfect electric conductors, while the internal plastic parts and the radome were modeled as lossy dielectric material ($\varepsilon_r = 4.3$, $\sigma = 0.001$ S/m). The radiating elements were excited in the simulation at the direct location of the connecting cables and the feeding network was not modeled, which means that the internal losses were not included in the simulation. The antenna under investigation has a double cross-polarization of $+45^\circ$ and -45°, which provides diversity in a space-efficient manner. This means that many significant parts of the antenna are at a 45° angle to the main axes of the antenna, which required the spatial discretization of the computational grid to be relatively fine—the smallest steps were <0.5 mm.

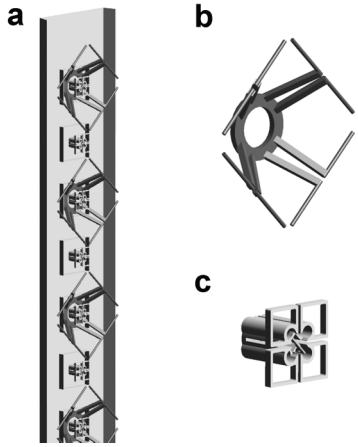

Fig. 1. Internal structure of the antenna. Top half of the antenna array is shown on the left (**a**); GSM 900 radiating element (**b**) and GSM 1800/UMTS radiating element (**c**) are shown on the right. Internal plastic parts for structural reinforcement were included in the model but are not shown in this figure.

Two excitation schemes were evaluated and compared to published measurement results [Toivonen et al., 2009]. The accuracy of the antenna model in free space was also evaluated by comparing calculated far-field radiation patterns with the far-field data from the antenna manufacturer. In the first scheme, all radiating elements were excited with the same signal, using a voltage source at 1 V amplitude as used previously by Gosselin et al. [2009]. In the second scheme, however, the elements were excited at a constant phase, but at relative amplitudes of 0.54, 0.78, 1, 1, 0.78, and 0.54 (as reported by van Wyk et al. [2005]), with the relative amplitude 1 applied to the elements in the center of the antenna (two center-most elements at 900 MHz and three center-most elements at 1800 and 2100 MHz). After the simulation, the resulting fields were normalized to 1 W radiated power. Both excitations used a constant phase between the elements because more accurate phase distribution between the elements was not available.

Before calculating SAR in the human models, we had validated our antenna model. Several simulations were performed and compared with published measurements, first in free space, and then with a box phantom (500 mm × 800 mm × 200 mm) as detailed in the CENELEC 50383 standard [CENELEC, 2002]. For the free-space simulations, the FDTD grid was padded with 800 mm of background in the direction of the main beam, and to 4λ in the other directions. The E field was then calculated and the maximum value of E_{RMS} was obtained in the planes parallel to the antenna surface at distances of 10, 100, 300, and 600 mm; this method corresponds very well to the plane sweep measurement described in CENELEC [2002] and Toivonen et al. [2009].

Localized spatial-peak SAR (henceforth: SAR_{10g}) in the box phantom fluid was calculated at the aforementioned distances between the phantom and the antenna and compared to measurements of the same antenna published in the literature [Toivonen et al., 2009]. The relative permittivities of the phantom fluid were 38.1, 39.4, and 34.8 for GSM 900, GSM 1800, and UMTS, respectively, and the electric conductivities were 0.99, 1.4, and 1.56 S/m for GSM 900, GSM 1800, and UMTS, respectively. For each point examined, a cube was used as the averaging volume for SAR_{10g} with an algorithm according to the IEEE C95.3 standard [IEEE, 2002].

Human Model

We used the Virtual Family male and female anatomical human models [Christ et al., 2010]. They represent an average European male and female, with a height of 1.74 and 1.6 m, respectively, and a mass of 70 and 58 kg, respectively. The body mass indexes of the two models are very similar: 23.1 for the male model and 22.7 for the female. Tissue parameters were evaluated from the well-known parametric model [Gabriel et al., 1996b] for each center frequency used in the simulations.

The simulations were performed for three separate setups at five different distances between the antenna and body measured in the normal direction from the front of the antenna radome. The male model was simulated in two positions: (i) with the head near the center of the antenna, so as to represent the worst case for SAR_{10g} in the head, and (ii) with the body at the same height as the antenna, to represent the worst case for whole-body SAR (henceforth: SAR_{wb}). The female model was positioned in a manner similar to the second male position.

In all cases, the body was positioned facing the antenna, oriented in such a way that the distance between the antenna and the body was perpendicular to the antenna's long axis and was kept as constant as possible. The distances are therefore shortest at the nose, and longer, for example, at the neck and the legs. The only exception to this is the feet, which are turned forward in the model; the toes are therefore closer to the antenna than the rest of the body. The different positions of the human models in front of the antenna are illustrated in Figure 2.

Evaluating Combined Exposure

The ICNIRP Guidelines [ICNIRP, 1998] give the following formula for determining whether the basic restrictions have been exceeded in the case of combined

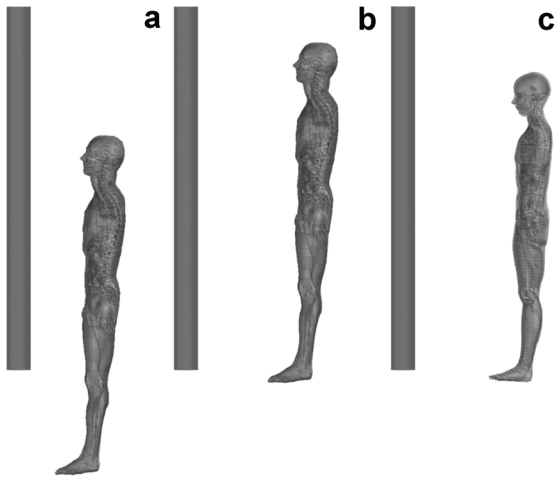

Fig. 2. Illustration of the different positions of the models in front of the antenna. Positions 1 (**a**) and 2 (**b**) of the male model are shown on the left. The female model was positioned similar to male 2, with the feet at the same height (**c**).

exposure:

$$\sum_i \frac{\mathrm{SAR}_i(f_i)}{\mathrm{SAR}_\mathrm{L}(f_i)} \leq 1$$

where SAR_i is SAR caused by the field at frequency f_i and SAR_L is the basic restriction. The guidelines specify that the effects of the fields of different frequencies should be examined for additivity, and if they are found to be additive, the maximum value of SAR at each frequency should be used. With $\mathrm{SAR}_{\mathrm{wb}}$, this is the only possibility, as it is an integrated value over the whole body. $\mathrm{SAR}_{10\mathrm{g}}$, however, is aimed at preventing small localized heat stress in tissues. If there are several hot-spots in the body, all of them caused by the same frequency and all below the basic restriction, the exposure is within the limits. However, if the hot-spots are caused by different frequencies, then each of them being below the basic restriction is not necessarily sufficient because the sum in the formula above could still exceed 1.

To evaluate the combined exposure and explore the additivity of $\mathrm{SAR}_{10\mathrm{g}}$ in the case of the three-band base station antenna in more detail, we summed the $\mathrm{SAR}_{10\mathrm{g}}$ values voxel by voxel using the following algorithm. First, an FDTD simulation for each frequency present in the case under investigation was run. To enable the results to be added in a simple manner, without requiring further interpolation of data, the same computational grid was used in all simulations. Next, the $\mathrm{SAR}_{10\mathrm{g}}$ values were extracted and normalized to the total power of each frequency. The contributions from each frequency were then added together voxel by voxel. Finally, the maximum $\mathrm{SAR}_{10\mathrm{g}}$ was determined from the sum of all contributing frequencies and this was compared with the basic restrictions.

We used the efficient averaging algorithm based on IEEE C95.3 standard [IEEE, 2002], which is included in the SEMCAD package. In comparison to the more general requirement that the tissue over which the SAR is averaged only has to be contiguous, the averaging volume in the IEEE standard is more precisely defined (a cube) and thus more broadly comparable. The averaging speed is also crucial because very big meshes are required to simulate whole humans, and in order to find the global maxima the algorithm has to be applied to each voxel in the simulation.

In evaluating the combined effects of the three different frequencies, it is necessary to keep in mind that in general, the different bands will have different total radiated powers. In total, eight different distributions of radiated power among the three frequencies were investigated, with the ratios of power between GSM 900, GSM 1800 and UMTS being the following, respectively: 1–1–1, 1–2–2, 1–2–5, 2–3–5, 2–3–1, 2–2–5, 5–3–2, and 5–3–5. To enable a direct comparison between results with a different total radiated power, we normalized all results to 1 W.

RESULTS

Antenna Model Validation

In order to validate our numerical model, we compared the simulated free-space far-field pattern with the manufacturer's data, and good agreement was obtained for the non-uniform excitation scheme: the differences in the vertical half-power beamwidth were 0.5°, 0.1°, and 0° at 900, 1800, and 2100 MHz, respectively, and the differences in the maximum gain were 1.1, 0, and 1.8 dB at 900, 1800, and 2100 MHz, respectively. Furthermore, we compared the results of our simulations to previously published data [Toivonen et al., 2009], both for free-space maximum E_{RMS} and for $\mathrm{SAR}_{10\mathrm{g}}$ inside a standardized box phantom. The results are presented in Table 1. With respect to

TABLE 1. Comparison Between Simulated and Measured Values

Distance (mm)	GSM 900			GSM 1800			UMTS		
	Meas.[a]	Sim.	Diff. (%)	Meas.[a]	Sim.	Diff. (%)	Meas.[a]	Sim.	Diff. (%)
E_{max} (V/m RMS)									
10	46.7	56.5	21	54.9	62.7	14	65.2	80.9	24
100	32.2	38.3	19	40.3	40.4	0	46.2	49.9	8
300	20.3	27.3	34	24.7	32	30	29.8	31.4	5
600	17	21	24	18.7	23.5	26	21.7	22.3	3
$\mathrm{SAR}_{10\mathrm{g}}$ (W/kg)									
10	0.230	0.236	2	0.235	0.260	11	0.355	0.474	33
100	0.058	0.086	49	0.088	0.098	11	0.202	0.241	20
300	0.017	0.030	76	0.066	0.060	−9	0.047	0.062	32
600	0.012	0.020	70	0.020	0.027	36	0.035	0.045	28

The presented E values are the maximum measured or simulated E_{max} (V/m RMS) in a plane sweep measurement at different distances from the antenna, while the SAR values represent the maximum measured or simulated $\mathrm{SAR}_{10\mathrm{g}}$

[a]Published in Toivonen et al. [2009].

the non-uniform excitation scheme, the results for the first excitation (with all amplitudes equal to 1) were, on average, 15% lower for the *E* field, and up to 40% lower for SAR. The non-uniform excitation scheme was finally selected for the human model calculations and the uncertainty analysis was based on that excitation scheme. The uncertainties of the antenna model are discussed below. The simulated field is shown on the slice plot in Figure 3. The slices pass through the middle of the antenna and present a side view of the panel.

Error Analysis

Among all 24 data points, comparing simulations and measurements in Table 1, the largest error of our simulations was 2.6 dB, while the error was smaller than 2 dB in more than 80% of the cases. Based on these errors and the uncertainty of the original measurement setup (approximately 1 dB for extended uncertainty, based on a similar setup described by Kuster et al. [2006]), a conservative estimate of the errors of the model is 3.2 dB, systematically in the direction of overestimating the actual exposure. The contributions to the uncertainty are the following: unknown excitation scheme used in the actual antenna (i.e., differences in power fed to each element and also each element's relative phase); internal losses in the real antenna that reduce the total radiated power by an unknown amount; difference in matching between different elements at the same frequency; and the unknown effect of the proximity of conductive bodies on the feeding network and power distribution between different radiating elements.

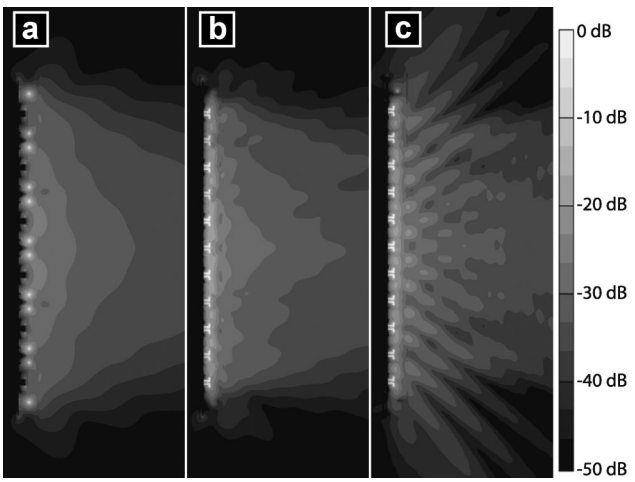

Fig. 3. E_{RMS} in the center plane of the antenna at 1 W total radiated power. From left to right are fields at (**a**) 900 MHz, (**b**) 1800 MHz, and (**c**) 2100 MHz. The scale is in dB, and 0 dB corresponds to 1000 V/m.

The values of SAR in the human model are further influenced by uncertainties in tissue dielectric parameters [Gabriel et al., 1996a] and to a small extent by the number of FDTD cells per wavelength in the FDTD simulation (only at 2100 MHz). The number of FDTD cells per wavelength does increase the numerical propagation speed error by a small amount [Taflove and Hagness, 2005]; however, it is still small with respect to the uncertainties in dielectric properties of body tissue [Gabriel et al., 1996a], in particular its permittivity. The uncertainties in permittivity have a greater effect when SAR_{10g} values are low compared to the SAR_{wb}, or when the errors are involved in tissues that form a large part of the model (e.g., muscle) [Mason et al., 2000; Gajsek et al., 2001a,b].

Human Exposure

The results for human exposure are presented in Table 2, which lists the percentage of basic restriction per 1 W of transmitted power. SAR_{10g} in the UMTS frequency band reaches the highest level—5.41%/W at 10 mm from the antenna for the male model in position 2. SAR_{10g} is the highest at 2100 MHz in most other cases as well. This is expected since the body absorbs higher frequencies in a smaller volume; thus, for a similar total absorbed power, the average power in a constant volume is larger.

For SAR_{wb}, all the three frequencies result in a similar exposure. Since the antenna in the study is larger than the human models used in the study, the energy is absorbed almost uniformly across the whole body. Therefore, the localized SAR_{10g} is the more restrictive constraint up to distances of about 200 mm. At larger distances, SAR_{wb} is the more limiting factor. The results of combined exposure are presented in Table 3. The comparison of the two summation approaches in Table 4 shows that the largest difference between them is 55% for the female model at 200 and 500 mm from the antenna (50–30–20% power ratio). The median value of all the computed differences (they are not normally distributed) was 18.5%, with the 25th and 75th percentile being 11% and 27%, respectively.

In the case of occupational exposure to base station antennas, some tissues have a higher average exposure than others. While the maximum peak values are always found in the tissues closest to the surface of the body, such as skin or muscle, some internal organs also receive a high exposure relative to their mass. We have computed SAR statistics for each different tissue in the model, and the highest mean SAR values over the entire tissue were found in the cornea, larynx, penis, sclera, thyroid gland, and testes. These tissues all have a low total mass, so the average SAR over the

TABLE 2. Simulated Values of SAR in % of Basic Restriction (10 W/kg for SAR_{10g} and 0.4 W/kg for SAR_{wb}) per Watt of Total Radiated Power

	GSM 900 only			GSM 1800 only			UMTS only		
Distance (mm)	Male 1	Male 2	Female	Male 1	Male 2	Female	Male 1	Male 2	Female
SAR_{10g}									
10	2.25	2.96	1.45	3.18	3.25	2.99	3.81	5.41	3.04
100	1.15	1.27	1.03	2.33	1.79	1.60	2.94	1.74	1.65
200	0.87	1.13	0.96	1.08	1.77	1.03	1.10	1.37	1.11
500	0.48	0.55	0.56	0.65	0.58	0.51	0.62	0.63	0.64
1000	0.26	0.31	0.42	0.40	0.45	0.41	0.47	0.37	0.39
SAR_{wb}									
10	1.66	2.33	2.95	1.52	2.18	2.45	1.68	2.30	2.45
100	1.28	1.75	2.36	1.21	1.77	2.05	1.15	1.63	1.70
200	1.10	1.58	2.06	1.00	1.39	1.55	0.93	1.28	1.50
500	0.71	0.96	1.32	0.69	0.98	1.13	0.67	0.94	1.04
1000	0.43	0.59	0.81	0.43	0.63	0.69	0.38	0.51	0.57

The values for SAR_{10g} and SAR_{wb} at each frequency are shown separately

whole tissue can reach more than 50% of the maximum SAR_{10g}.

DISCUSSION

We have presented a calculation of the occupational exposure in front of a multi-band base station antenna. Prior to calculating exposure in anatomical human models, we have conducted an extensive validation of the model by comparing our results to previously published studies. This comparison shows that our approach gives a good estimation of the SAR inside a standardized phantom [CENELEC, 2002], even at close distances. The fact that the results are biased toward overestimating the exposure is related to the choice of excitation of the separate antenna elements. Namely, we have chosen a symmetrical, non-uniform excitation amplitude at different radiating elements, as described by van Wyk et al. [2005], rather than an identical amplitude at each element, with the goal of obtaining better results in the closest vicinity of the antenna. Another source of discrepancy is the fact that the internal feeding network of the antenna was not modeled and, therefore, the internal losses of the antenna are not taken into account. Since the measurements [Toivonen et al., 2009] were normalized to 1 W input power to the antenna, and our simulations are normalized to 1 W total radiated power, the difference between the two should be taken into account. However, since the exact internal losses are unknown, they cannot be separated from other sources of errors in the evaluation.

At larger distances, the SAR_{wb} is the more limiting factor in our results as well as in previously published literature [Thors et al., 2008; Gosselin et al., 2009], especially when large antennas are considered. The close distance between the antenna and the body affects the impedance of the radiating elements and thus the matching. The resulting change in the antenna feed structure has been studied previously, and has been found to influence the calculated values of SAR [Joseph and Martens, 2005; van Wyk et al., 2005]. Our validation (Table 1) shows that the model does not underestimate the SAR even at the smallest antenna–phantom distances. The largest difference between measurements and our simulated results was 2.6 dB, which may be partly caused by less than ideal matching of the radiating elements (average SWR was 1.58, 1.5, and 4.5 at 900, 1800 and 2100 MHz, respectively).

The results of the simulations performed on the anatomical model show that the occupational exposure to a single frequency is the highest at 2100 MHz for localized SAR_{10g}, but for the SAR_{wb} none of the frequencies plays such a dominant role, with all three frequencies contributing very similarly to exposure in each of the three cases examined. The differences between exposures for the male (position 2) and the female model in SAR_{10g} are not very large, but the female does have a higher exposure for SAR_{wb}. This can be explained by the smaller weight of the female model; although the total power absorbed by the female is slightly lower than by the male, the ratio of power to mass, and thus SAR_{wb}, is larger in the end.

In evaluating the simultaneous exposure, we compared two different summation approaches: a simple method of summation of the maxima, and a much more demanding voxel-by-voxel summation. The largest difference in the results caused by the difference in the summation approach is 55% in the female model

TABLE 3. Comparison of Voxel-by-Voxel Summation at Different Ratios of Transmitted Power Power (GSM 900–GSM 1800–UMTS 2100)

	Combined SAR_{10g} (power ratio)							
Distance (mm)	1–1–1	1–2–2	1–2–5	2–3–5	2–3–1	2–2–5	5–3–2	5–3–5
Male 1								
10	2.42	2.70	3.11	2.84	2.38	2.88	2.04	2.43
100	1.89	2.18	2.46	2.24	1.80	2.24	1.55	1.84
200	0.83	0.88	0.96	0.90	0.80	0.90	0.77	0.83
500	0.44	0.47	0.49	0.46	0.48	0.47	0.42	0.42
1000	0.32	0.36	0.40	0.37	0.31	0.36	0.27	0.31
Male 2								
10	3.27	3.34	3.95	3.55	3.16	3.68	3.15	3.30
100	1.52	1.61	1.65	1.60	1.54	1.58	1.42	1.48
200	1.07	1.08	1.09	0.99	1.26	1.02	1.12	1.00
500	0.52	0.52	0.55	0.53	0.51	0.54	0.51	0.52
1000	0.36	0.38	0.37	0.37	0.37	0.36	0.34	0.34
Female								
10	2.06	2.33	2.54	2.36	2.03	2.34	1.72	1.99
100	1.21	1.36	1.46	1.37	1.20	1.35	1.03	1.16
200	0.73	0.78	0.88	0.82	0.69	0.84	0.65	0.74
500	0.42	0.47	0.53	0.49	0.39	0.50	0.36	0.42
1000	0.28	0.32	0.34	0.32	0.28	0.32	0.29	0.27
	Combined SAR_{wb}							
Distance (mm)	1–1–1	1–2–2	1–2–5	2–3–5	2–3–1	2–2–5	5–3–2	5–3–5
Male 1								
10	1.62	1.61	1.64	1.63	1.59	1.64	1.62	1.64
100	1.22	1.20	1.18	1.20	1.23	1.19	1.24	1.22
200	1.01	0.99	0.97	0.98	1.02	0.98	1.04	1.01
500	0.69	0.69	0.68	0.68	0.70	0.68	0.70	0.69
1000	0.42	0.41	0.40	0.41	0.42	0.41	0.42	0.41
Male 2								
10	2.27	2.26	2.27	2.27	2.25	2.28	2.28	2.28
100	1.72	1.71	1.68	1.70	1.74	1.69	1.73	1.71
200	1.42	1.39	1.35	1.37	1.44	1.37	1.47	1.42
500	0.96	0.96	0.95	0.96	0.97	0.95	0.96	0.96
1000	0.58	0.57	0.55	0.56	0.59	0.55	0.58	0.57
Female								
10	2.62	2.55	2.51	2.55	2.62	2.56	2.70	2.64
100	2.04	1.98	1.87	1.94	2.10	1.93	2.14	2.04
200	1.70	1.63	1.58	1.63	1.71	1.64	1.79	1.73
500	1.17	1.14	1.10	1.13	1.18	1.13	1.21	1.17
1000	0.69	0.67	0.63	0.66	0.71	0.65	0.73	0.69

All results are shown in % of basic restriction (10 W/kg for SAR_{10g} and 0.4 W/kg for SAR_{wb}) and are normalized to 1 W total radiated power.

(at 200 and 500 mm distances). This shows that for similar designs of collinear multi-band base station antennas, where the radiating elements of different frequencies are packed close together, the peaks of energy absorption tend to be located at similar spots in the human body, also at different frequencies. The combined SAR_{10g} exposure is dominated by the highest frequency present—in this case, 2100 MHz. The additivity is also illustrated in Figure 4, where a separate comparison between each frequency band and a combined exposure is presented. Since the difference between the voxel-by-voxel summation and the much simpler summation of maxima is relatively small, the simple approach can be recommended for investigations of compliance with the basic restrictions. The voxel-by-voxel summation requires much more storage and computational power. To calculate the maximum SAR for a different ratio of powers at the antenna, it is necessary to store the data for SAR for the whole-body volume for each frequency (for FDTD, this represents a 3D array with as many elements as the number of tissue voxels), and then find the maximum element of the

TABLE 4. Overestimation of Combined SAR by the Simple Summation Approach

	Combined SAR_{10g} (power ratio), %							
Distance (mm)	1–1–1	1–2–2	1–2–5	2–3–5	2–3–1	2–2–5	5–3–2	5–3–5
Male 1								
10	27	20	11	17	25	15	40	26
100	13	7	4	7	13	7	20	15
200	22	19	11	16	26	15	27	21
500	33	30	23	30	22	26	33	35
1000	18	11	7	11	18	11	26	19
Male 2								
10	18	21	15	20	11	19	12	20
100	5	4	2	4	5	4	7	6
200	33	37	32	46	18	38	22	37
500	13	13	10	12	14	11	13	13
1000	5	3	2	3	5	4	7	6
Female								
10	21	16	11	15	23	14	30	21
100	17	10	7	10	18	11	29	20
200	41	34	21	28	47	26	55	39
500	34	22	12	19	40	19	55	36
1000	43	27	16	25	45	26	43	48

voxel-wise sum of these arrays weighted by appropriate radiated powers. Additionally, these SAR values will be true for only one orientation of the body and may not necessarily be the same in a different orientation.

For the presented antenna, the worst-case exposures can be evaluated for each distance from the antenna (both SAR_{10g} and SAR_{wb}) and from these, the maximum total radiated power that will not cause the basic restrictions to be exceeded can be determined. Taking into account the estimated error of 3.6 dB, these powers are 8, 15, 21, 33, and 54 W at 10, 100, 200, 500, and 1000 mm, respectively. It is important to note that these are actual transmitted powers at the antenna and they should take into account the losses in the antenna feed cables, internal losses in the antenna, and losses in combiners and other equipment at a base station site.

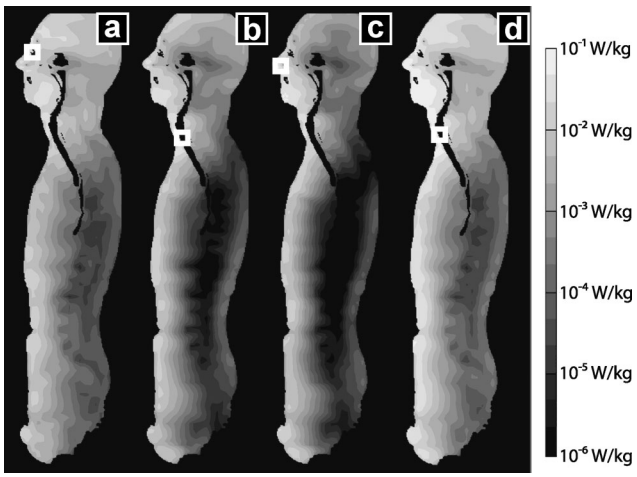

Fig. 4. SAR_{10g} in the male model at 500 mm from the antenna. From left to right are: (**a**) 900 MHz, (**b**) 1800 MHz, (**c**) 2100 MHz, and (**d**) voxel-by-voxel combined SAR values for all three frequencies. The white squares indicate the location of the maximum values of SAR_{10g}. The ratios of power for each frequency are 1–1–1, and the total radiated power of all frequencies is 3 W.

In the case of combined, multi-band exposure, as well as for single frequencies, the SAR_{wb} is the more limiting factor at larger distances (above 200 mm), while SAR_{10g} becomes more restrictive at smaller distances. Similar results were obtained in previous studies [Martinez-Burdalo et al., 2005; Gosselin et al., 2009], although they only examined exposure to one frequency at a time.

CONCLUSIONS

In evaluating simultaneous exposure to several frequencies emitted by a multi-band antenna, where there are several linear arrays one within the other, a simple summation of highest spatial-peak SAR values for each frequency provides a good, slightly conservative approximation of the real combined SAR. Using this approach, it is also very easy to calculate the exposure levels for different transmitting powers of the antenna in different real-life situations, so this should be the preferable method in assessing occupational exposure according to current legislation.

ACKNOWLEDGMENTS

The authors would like to thank Mobitel for providing access to the antenna presented in this work.

REFERENCES

Ackerman MJ. 1998. The visible human project. Proc IEEE 86:504–511.

CENELEC. 2002. Basic standard for the calculation and measurement of EMF strength and SAR related to human exposure from radio base stations and fixed terminal stations for wireless telecommunications systems (110 MHz–40 GHz). European Standard EN 50383. Brussels, Belgium; CENELEC.

Christ A, Kainz W, Hahn E, Honegger K, Zefferer M, Neufeld E, Rascher W, Janka R, Bautz W, Chen J, Kiefer B, Schmitt P, Hollenbach H, Shen J, Oberle M, Szczerba D, Kam A, Guag J, Kuster N. 2010. The Virtual Family-development of surface-based anatomical models of two adults and two children for dosimetric simulations. Phys Med Biol 55:N23–N38.

Cooper J, Marx B, Buhl J, Hombach V. 2002. Determination of safety distance limits for a human near a cellular base station antenna, adopting the IEEE standard or ICNIRP guidelines. Bioelectromagnetics 23:429–443.

Dimbylow PJ. 1997. FDTD calculations of the whole-body averaged SAR in an anatomically realistic voxel model of the human body from 1 MHz to 1 GHz. Phys Med Biol 42:479–490.

Faraone A, Tay RYS, Joyner KH, Balzano Q. 2000. Estimation of the average power density in the vicinity of cellular base-station collinear array antennas. IEEE Trans Vehicular Tech 49:984–996.

Gabriel S, Lau RW, Gabriel C. 1996a. The dielectric properties of biological tissues: III. Parametric models for the dielectric spectrum of tissues. Phys Med Biol 41:2271–2293.

Gabriel S, Lau R, Gabriel C. 1996b. The dielectric properties of biological tissues: II. Measurements in the frequency range 10 Hz to 20 GHz. Phys Med Biol 41:2251–2269.

Gajsek P, Hurt WD, Ziriax JM, Mason PA. 2001a. Parametric dependence of SAR on permittivity values in a man model. IEEE T Bio-Med Eng 48:1169–1177.

Gajsek P, Ziriax JM, Hurt WD, Walters TJ, Mason PA. 2001b. Predicted SAR in Sprague–Dawley rat as a function of permittivity values. Bioelectromagnetics 22:384–400.

Gosselin MC, Christ A, Kuhn S, Kuster N. 2009. Dependence of the occupational exposure to mobile phone base stations on the properties of the antenna and the human body. IEEE Trans Electromagn Compat 51:227–235.

Hand JW. 2008. Modelling the interaction of electromagnetic fields (10 MHz–10 GHz) with the human body: Methods and applications. Phys Med Biol 53:R243–R286.

ICNIRP. 1998. Guidelines for limiting exposure to time-varying electric, magnetic, and electromagnetic fields (up to 300 GHz). Health Phys 74:494–522.

IEEE. 2002. IEEE Recommended Practice for Measurements and Computations of Radio Frequency Electromagnetic Fields With Respect to Human Exposure to Such Fields, 100 kHz-300 GHz. IEEE Std C95. 3-2002 (Revision of IEEE Std C95.3-1991).

IEEE. 2006. IEEE Standard for Safety Levels with Respect to Human Exposure to Radio Frequency Electromagnetic Fields, 3 KHz to 300 GHz. IEEE Std C95. 1-2005 (Revision of IEEE Std C95.1-1991).

Joseph W, Martens L. 2005. Comparison of safety distances based on the electromagnetic field based on the SAR for occupational exposure of a 900-MHz base station antenna. IEEE Trans Electromagn Compat 47:977–985.

Kuster N, Torres VB, Nikoloski N, Frauscher M, Kainz W. 2006. Methodology of detailed dosimetry and treatment of uncertainty and variations for in vivo studies. Bioelectromagnetics 27:378–391.

Lacroux F, Conil E, Carrasco AC, Gati A, Wong MF, Wiart J. 2008. Specific absorption rate assessment near a base-station antenna (2,140 MHz): Some key points. Ann Telecommun 63:55–64.

Martinez-Burdalo M, Martin A, Anguiano M, Villar R. 2005. On the safety assessment of human exposure in the proximity of cellular communications base-station antennas at 900, 1800 and 2170 MHz. Phys Med Biol 50:4125–4137.

Mason P, Hurt W, Walters T, D'Andrea J, Gajsek P, Ryan K, Nelson D, Smith K, Ziriax J. 2000. Effects of frequency, permittivity, and voxel size on predicted specific absorption rate values in biological tissue during electromagnetic-field exposure. IEEE Trans Microwave Theor Tech 48:2050–2058.

Taflove A, Hagness SC. 2005. Computational electrodynamics: The finite-difference time-domain method. 3rd edition. Norwood, MA: Artech House.

Thors B, Strydom ML, Hansson B, Meyer FJC, Karkkainen K, Zollman P, Ilvonen S, Tornevik C. 2008. On the estimation of SAR and compliance distance related to RF exposure from mobile communication base station antennas. IEEE Trans Electromagn Compat 50:837–848.

Toivonen T, Toivo T, Puranen L, Jokela K. 2009. Specific absorption rate and electric field measurements in the near field of six mobile phone base station antennas. Bioelectromagnetics 30:307–312.

van Wyk MJ, Bingle M, Meyer FJC. 2005. Antenna modeling considerations for accurate SAR calculations in human phantoms in close proximity to GSM cellular base station antennas. Bioelectromagnetics 26:502–509.